A Compact High-Gain Dual-Circularly Polarized Antenna Based on High-Order Mode Microstrip Patch

Dieu Nguyen-Khanh, Dat Nguyen-Tien, Nguyen Tran, Thai Dinh Nguyen, Niamat Hussain, and Hung Tran-Huy

***Abstract*—This paper presents a method to design a high-gain dual circularly polarized (CP) antenna with compact size based on high-order mode patch structure. For high-gain radiation, a square patch is excited to operate in high-order TM03 mode. To suppress grating lobes and reduce the overall size, four open slots are etched on the edges of the patch. For dual-CP realization, a 90° hybrid coupler is employed as the feeding network. By changing the feeding port, either right-hand CP (RHCP) or left-hand CP (LHCP) with high isolation can be produced. An antenna prototype with overall dimensions of $1.49\,\lambda \times 1.49\,\lambda \times 0.04\,\lambda$ at 5.6 GHz is fabricated and measured for validation. The measurements demonstrate that the proposed design achieves good dual-CP performance around 5.6 GHz with a peak realized gain of approximately 12 dBi. In comparison with the high-gain dual-CP antennas using array or Fabry-Perot structures, the proposed approach has the advantage of achieving high gain with a compact and simple configuration.**

Link to graphical and video abstracts, and to code:
https://latamt.ieeer9.org/index.php/transactions/article/view/10388

***Index Terms*—Patch antenna, circular polarization, high-order mode, high gain, dual-CP.**

I. Introduction

CIRCULARLY polarized (CP) antennas have been widely used since they can reduce polarization mismatch and mitigate multipath interference in communication and navigation systems. Besides, CP antennas with the capability of radiating both right-hand CP (RHCP) and left-hand CP (LHCP) have the advantages of providing polarization diversity, improving link robustness, as well as spectral utilization. Conventional dual-CP microstrip antennas are typically realized by exciting two orthogonal fundamental modes (TM_{10} and TM_{01}) using either two orthogonal feeds with a 90° phase shift or an external branch-line hybrid coupler [1]–[8]. However, because these antennas are based on the fundamental mode with a small effective radiating aperture, they inherently suffer from limited radiation gain, which is typically lower than 8.0 dBi. This drawback restricts their application in long-range wireless links.

For high-gain realization, a thorough investigation in the open literature indicates three major approaches. The first is to construct a dual-CP antenna in an array configuration, in which multiple radiating elements are arranged in planar or sequential rotation to enlarge the effective radiating aperture. In [9]–[12], 4-element arrays can achieve a broadside gain of around 12 dBi. Better gain performance can be observed in [13]–[16], where an extremely high gain of about 25.8 dBi is reported with 64 array elements. However, arranging multiple radiating elements with a proper distance significantly increases the antenna's footprint. Furthermore, incorporating a large number of elements greatly increases the structural complexity of the antenna.

Alternatively, using a Fabry-Perot (F-P) cavity structure is the second approach for gain enhancement. This type of antenna generally employs a frequency-selective surface (FSS) or a partially reflective surface (PRS) above the radiator, forming a resonant leaky cavity that collimates the beam and increases directivity. Various dual-CP Fabry-Perot antennas have been reported in [17]–[20]. Despite their effectiveness in gain improvement, F-P structures typically result in high profile and/or large footprint, making them unsuitable for compact or low-profile devices. A third approach is to excite high-order modes of a patch antenna to enlarge its radiating aperture with a single-element configuration [21]–[24]. Nevertheless, the gain enhancement in these studies has only been implemented for either linearly or single CP radiation.

This paper proposes an approach to designing a dual-CP antenna with high-gain and compact-size features. Here, the high-gain realization is obtained by using the high-order TM_{03}/TM_{30} mode of a square patch, while dual-CP radiation is produced with the aid of a hybrid coupler. It is noted that despite using similar TM_{03} patch, the design in [24] focuses on high-gain antenna with only single polarization and compact size features. Meanwhile, the proposed work focuses on high-gain antenna with dual-CP. Measurements on the fabricated antenna prototype demonstrate that the proposed antenna can achieve stable operation at 5.6 GHz with high-gain radiation of 12 dBi and compact overall dimensions of 1.49 $\lambda\times$ 1.49 $\lambda\times$ 0.04 λ. Operating at 5.6 GHz, the proposed antenna is compatible with IEEE 802.11a/ac systems. Besides, high gain and dual-CP operation make it suitable for UAV

The associate editor coordinating the review of this manuscript and approving it for publication was Roberto S. Murphy (*Corresponding author: Hung Tran-Huy*).

D. Nguyen-Khanh, D. Nguyen-Tien, N. Tran, T. D. Nguyen, and Hung Tran-Huy are with the Faculty of Electrical and Electronic Engineering, PHENIKAA School of Engineering, PHENIKAA University, Hanoi 12116, Vietnam (e-mails: 21012907@st.phenikaa-uni.edu.vn, dat.nguyentien@phenikaa-uni.edu.vn, nguyen.tranvietduc@phenikaa-uni.edu.vn, thai.nguyendinh@phenikaa-uni.edu.vn, and hung.tranhuy@phenikaa-uni.edu.vn).

N. Hussain is with James Watt School of Engineering, University of Glasgow, Scotland, UK (e-mail: niamat.hussain@glasgow.ac.uk).

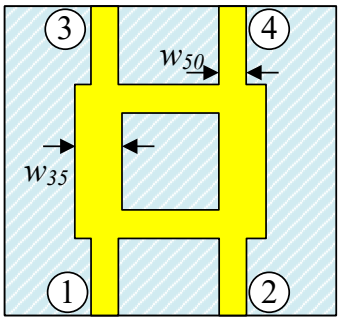

Fig. 1. Geometry of the 3-dB quadrature hybrid coupler, showing the branch-line layout for equal power division and 90° phase shift.

communications, point-to-point back-haul, where orientation robustness, multi-path mitigation, and long-range performance are critical.

II. Design of the Hybrid Coupler

The branch-line hybrid coupler is a four-port network that provides two output signals with equal amplitude and a 90° phase difference, while isolating the fourth port. Fig. 1 shows the geometry of the proposed 3-dB quadrature hybrid, which is employed to generate orthogonal excitations for dual circular polarization. In the conventional synthesis, the shunt arms are designed with a characteristic impedance of $Z_0 = 50\ \Omega$, whereas the series arms are implemented with $Z_0/\sqrt{2} \approx 35\ \Omega$, and all sections are a quarter-wavelength long at the design frequency [18]. The design is simulated and characterized using High Frequency Structure Simulator (HFSS).

After optimization, the coupler exhibits nearly equal power division of about -3 dB with a stable 90° phase difference at 5.6 GHz, as shown in Fig. 2. The simulated results also indicate excellent input matching, with return loss better than -20 dB and port isolation better than -40 dB. These characteristics confirm that the proposed hybrid coupler provides well-balanced excitations with high isolation, thereby enabling efficient generation of RHCP and LHCP in the antenna system.

III. Design of the Dual-CP Antenna

To enhance directivity while maintaining compactness, the square patch is designed to operate in the TM03 higher-order mode. The resonant length of the patch corresponding to the TM03 mode can then be approximated [25]:

$$W_p = \frac{3\lambda_{eff}}{2} = \frac{3c}{2f_r\sqrt{\varepsilon_{eff}}}, \tag{1}$$

where c is the speed of light in free space and f_r is the operating frequency. The patch is realized on a Taconic TLY-5 substrate with $\varepsilon_r = 2.2$, thickness $h = 1.52$ mm, and loss tangent of 0.0009. After optimization, the side length is chosen as $W_p = 52.3$ mm, corresponding to the TM03 resonance at 5.6 GHz. Two orthogonal probes are placed at (f_x, f_y) = (7.5 mm, 7.5 mm), and are excited by the quadrature hybrid coupler described in Section II, thereby enabling dual-sense CP radiation. The overall configuration of the high-order mode dual-CP patch antenna without slots is depicted in Fig. 3.

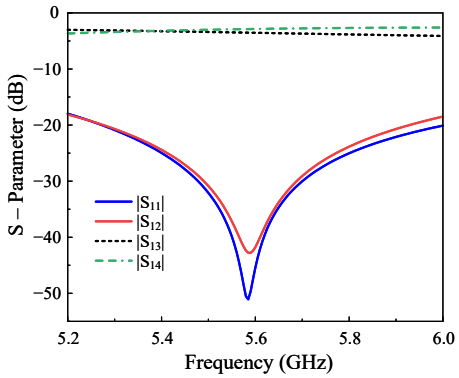

(a)

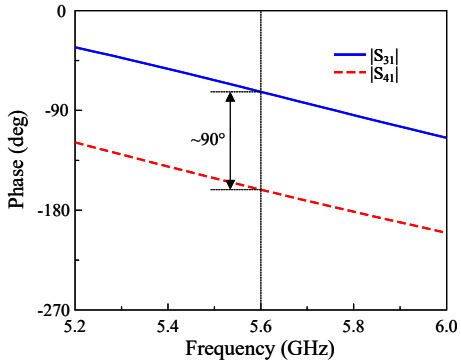

(b)

Fig. 2. Simulated (a) S-parameter and (b) Phase difference of the hybrid coupler.

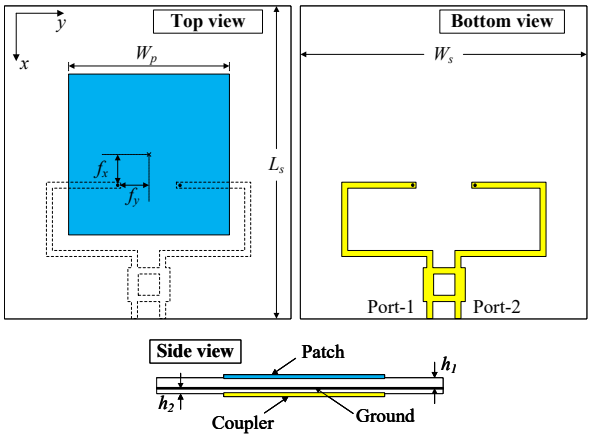

Fig. 3. Geometry of the high-order-mode dual-CP patch antenna, showing the patch layout and structural configuration.

The simulated results in Fig. 4 indicate that the antenna achieves good impedance matching around 5.6 GHz with a return loss of less than -20 dB. The realized gain reaches about 10.2 dBi, while the axial ratio remains under 3 dB around the desired frequency band. The gain and axial ratio are observed in the broadside direction. As illustrated in Fig. 5, strong grating lobes are observed in the radiation patterns, which are a typical feature of higher-order mode excitation.

Fig. 6 shows the simulated current distributions at 5.6 GHz on the patch with Port-1 excitation. It can be seen obviously that two orthogonal J-fields are produced at different phases.

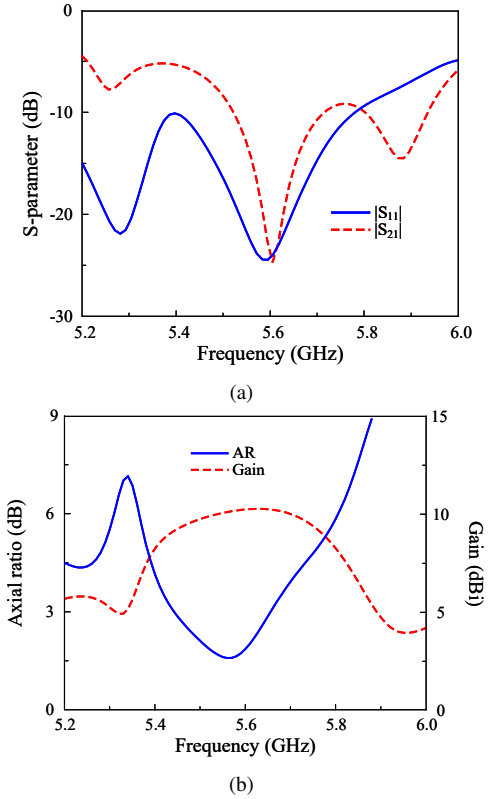

Fig. 4. Simulated (a) S-parameter, and (b) axial ratio (AR) and total gain of the high-order mode dual-CP patch antenna.

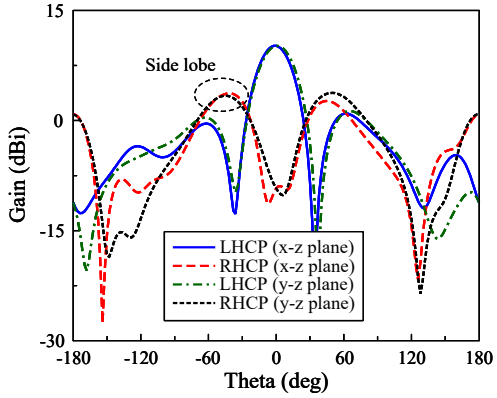

Fig. 5. Simulated gain radiation patterns of the high-order mode dual-CP patch antenna.

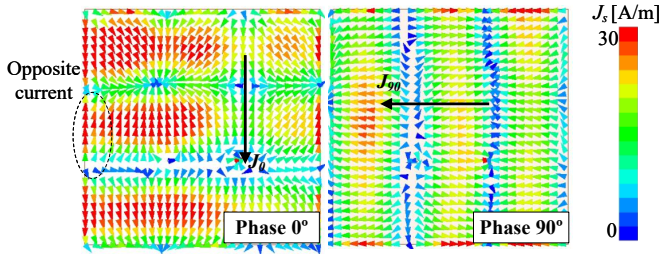

Fig. 6. Simulated surface current at 5.6 GHz for different phase angles, showing the rotating J-vectors that generate circular polarization.

When the phase changes from 0° to 90°, vector J rotates in a counterclockwise direction, which is evidence for RHCP

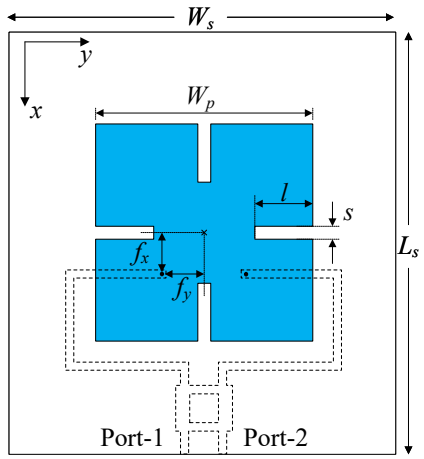

Fig. 7. Geometry of the high-order mode Dual-CP patch antenna with four open slots.

realization. The $TM_{30/03}$ mode is identified based on the simulated surface current, which exhibits three half-wavelength standing-wave variations along one principal dimension of the patch. This is characterized by three current maxima separated by two nulls with alternating current directions. Based on the current distribution shown in Fig. 6, it can be concluded that the presented antenna operates at $TM_{30/03}$ mode. Basically, the $TM_{30/03}$ mode turns a patch into a three-element in-phase/anti-phase radiator. The center part is out of phase to the others, which directly translates into pattern splitting and strong side-lobes. Regarding its contribution to the high gain, the $TM_{30/03}$ mode effectively enlarges the electrical aperture of the radiator. The radiation comes from a combination of two-element in-phase radiator, leading to high gain performance.

IV. High-Order Mode Dual-CP Antenna with Open Slots

To overcome the high grating lobe radiation, four open slots are later introduced on the patch surface, as shown in Fig. 7. In this design, the physical patch side is reduced to $W_p = 46$ mm. These slots effectively lengthen the current path, allowing the antenna to resonate at the desired frequency of 5.6 GHz while simultaneously suppressing grating lobes. The antenna is implemented on an 80 mm × 80 mm Taconic TLY-5 substrate with $\varepsilon_r = 2.2$, thickness $h = 1.52$ mm, and loss tangent of 0.0009. The optimized geometrical parameters are: feed offsets $f_x = f_y = 8.5$ mm, tuning length $l = 9.5$ mm, and slot spacing $s = 2.8$ mm.

Similar to the case without slots, the patch is excited via the 3-dB 90° hybrid coupler (Section II), which provides two orthogonal signals of equal amplitude and 90° phase difference to realize dual circular polarization. The simulated results confirm the advantages of the slot-loaded configuration. As shown in Fig. 8, the S-parameters ($|S_{11}|$, $|S_{21}|$) exhibit good impedance matching around 5.6 GHz, with $|S_{11}|$ lower than -20 dB and high port isolation of about 22 dB. The realized gain curve demonstrates a peak of approximately 12.3 dBi at

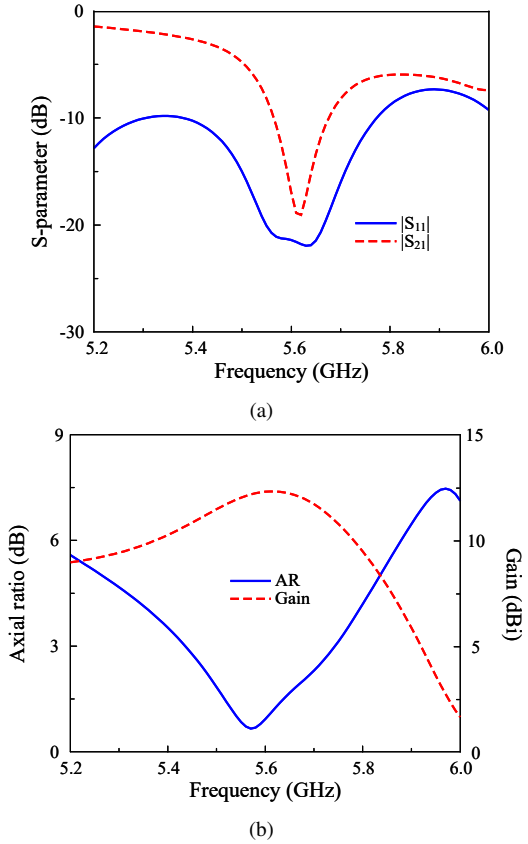

Fig. 8. Simulated (a) $|S_{11}|$ and $|S_{21}|$, (b) axial ratio (AR) and total gain of the high-order mode dual-CP patch antenna with four open slots.

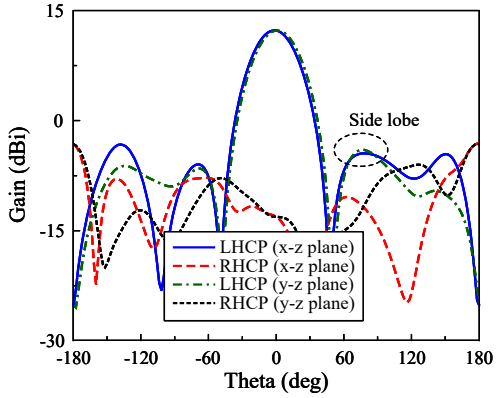

Fig. 9. Simulated gain radiation patterns of the high-order mode dual-CP patch antenna with four open slots.

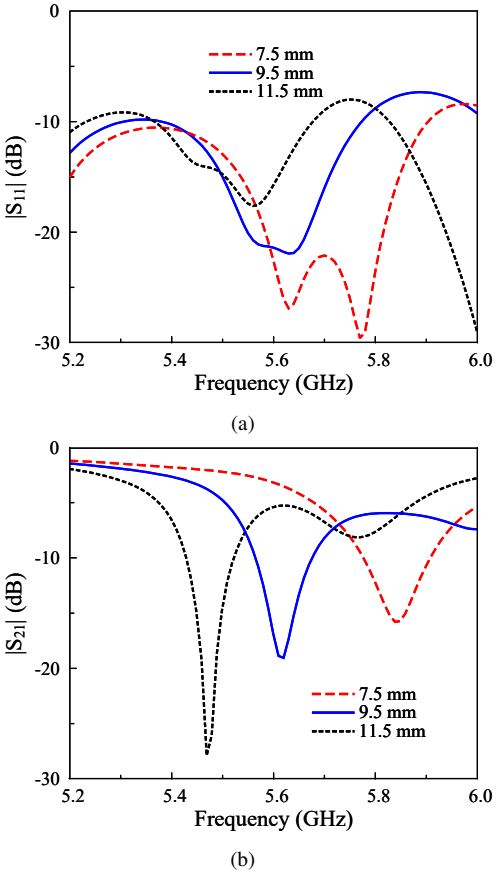

Fig. 10. Simulated (a) $|S_{11}|$ and (b) $|S_{21}|$ for different slot lengths, l.

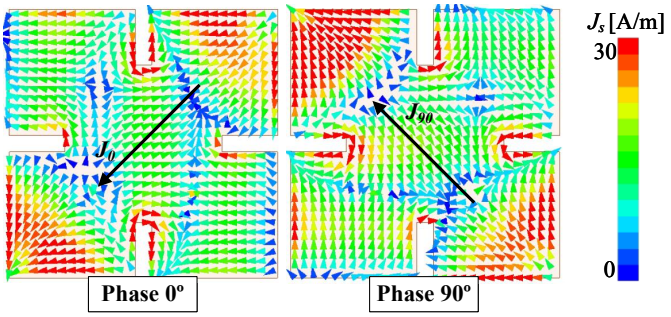

Fig. 11. Simulated surface current vectors on the slot-loaded patch at 5.6 GHz for different phase angles.

5.6 GHz, while the axial ratio remains below 3 dB across 5.45–5.75 GHz, ensuring stable circular polarization. Furthermore, Fig. 9 presents the radiation patterns, which clearly confirm the dual-CP operation with well-separated RHCP and LHCP beams and significantly reduced grating lobes compared to the no-slot case.

The effect of the sided slots on the antenna performance can be illustrated in Fig. 10. In terms of operating frequency, a longer slot results in a longer electrical length. Accordingly, the antenna operates at a lower frequency band. Finally, the simulated surface current distribution on the patch at 5.6 GHz with Port-1 excitation is presented in Fig. 11. Obviously, CP radiation can be generated when two orthogonal currents are produced at phase 0° and 90°. Besides, the counterclockwise rotation also demonstrates the RHCP radiation of the proposed patch. Meanwhile, there is no opposite current flowing on the patch, verifying the low sidelobe radiation of the proposed antenna. With the presence of the slots, the out of phase currents detour around the slots. These open slots radiate weakly. In the antenna, there are two in-phase currents, and then grating lobes are suppressed. It is also noted that the slot length is chosen so that the current detouring around the slot has total length of about half-guided wavelength at 5.6 GHz. The radiation is produced by a combination of two-element

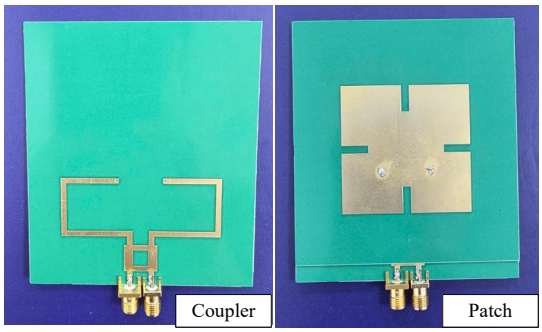

Fig. 12. Photographs of the fabricated antenna prototype, including both the front view and the back view.

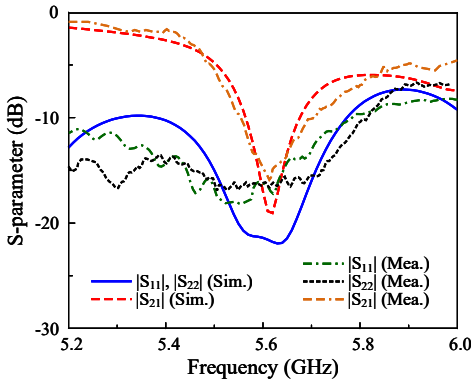

Fig. 13. Simulated and measured S-parameter of the proposed antenna.

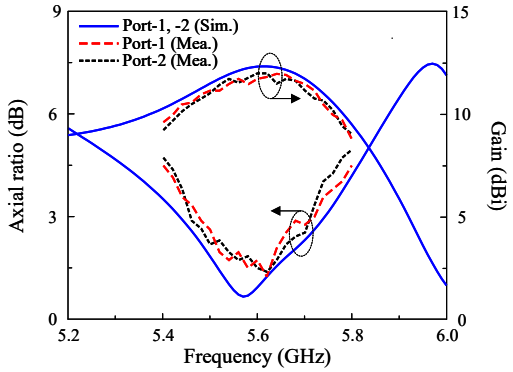

Fig. 14. Simulated and measured axial ratio and gain of the proposed antenna.

in-phase radiator, resulting in high gain performance.

V. Measurement Results

To assess the antenna's performance, an antenna prototype is fabricated and measured. Photographs of the fabricated prototype are presented in Fig. 12. In general, the measurement is well matched with the simulation. The difference might be attributed to tolerances in fabrication and measurement.

Fig. 13 shows the simulated and measured S-parameter of the proposed antenna. The simulated operating bandwidth with isolation of better than 10 dB is from 5.56 to 5.68 GHz, while the figure for measurement is from 5.55 to 5.7 GHz. The simulated and measured axial ratio of the fabricated

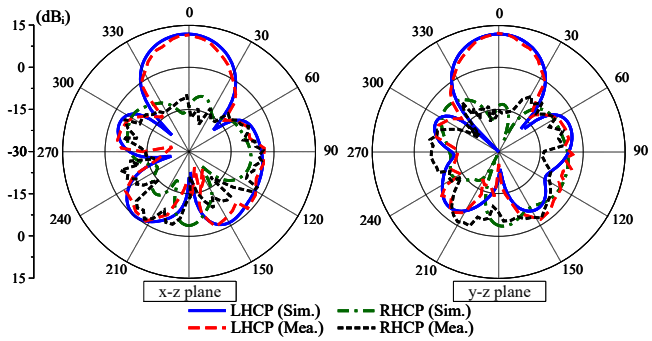

Fig. 15. Simulated and measured radiation patterns at 5.6 GHz with Port-1 operation.

antenna are illustrated in Fig. 14. It is noted that similar performance can be obtained for both Port-1 and Port-2. Across the operating bandwidth (5.55–5.7 GHz), the axial ratio is well below 3 dB. In terms of gain, the broadside gain shown in Fig. 14 is better than 11.0 dBi and achieves a maximum value of 12.0 dBi.

The measured and simulated radiation patterns at 5.6 GHz of the proposed antenna are plotted in Fig. 15. The radiation patterns in both principal planes reveal symmetrical main beams and good broadside radiation. The front-to-back ratio is about 18 dB in measurement. Meanwhile, the cross-polarization level is about -18.5 dB lower than the co-polarization level.

VI. Performance Comparison

Table I compares the performance of representative high-gain dual-CP antennas with the proposed design. Overall, it is obvious that the proposed antenna has the most compact size while achieving comparable gain. Compared to the array using four radiating elements [9]–[12], the proposed design exhibits higher gain, less complicated structure, and significantly lower profile than the antennas in [11], [12]. Meanwhile, using a large number of radiating elements in [13]–[16] can achieve higher gain, but at an extremely large size and complicated structures. In comparison with the gain improvement using Fabry-Perot structures [17]–[20], the proposed antenna has a smaller size and a significantly lower profile.

VII. Conclusion

A compact dual-CP antenna based on the excitation of higher-order TM30/TM03 modes has been proposed and experimentally validated. The prototype with compact dimensions of $1.49\,\lambda \times 1.49\,\lambda \times 0.04\,\lambda$ achieves a realized gain of 12.0 dBiC together with good impedance matching and an axial ratio below 3 dB across the band centered at 5.6 GHz. With its compact footprint, stable polarization purity, and ease of fabrication, the proposed antenna represents a practical low-profile solution for high-gain dual-CP radiation. It is therefore a promising candidate for integration into emerging wireless, satellite, and IoT systems where both miniaturization and polarization diversity are essential.

TABLA I
COMPARISON OF REPRESENTATIVE DUAL-CP ANTENNAS

Ref.	Method	Feeding mechanism	No. of elements	Dimensions (λ)	Gain (dBic)
[9]	Antenna array	Sequential rotation + multi-beam feed	$2 \times 2 = 4$	$2 \times 2 \times 0.2$	11.5
[10]	Antenna array	Cross-slot dual-feed + sequential-phase network	$2 \times 2 = 4$	$1.4 \times 1.4 \times 0.07$	11.22
[11]	Antenna array	3-dB power divider + DRA elements	$2 \times 2 = 4$	$1.82 \times 0.94 \times 0.14$	10
[12]	Antenna array	Printed ridge gap waveguide + branch-line coupler	$2 \times 2 = 4$	$1.15 \times 1.15 \times 0.45$	11.7
[13]	Antenna array	Corporate microstrip feed with quarter-wave dividers	$4 \times 4 = 16$	$2.92 \times 2.92 \times 0.083$ @ 28 GHz; $3.96 \times 3.96 \times 0.113$ @ 38 GHz	18.5
[14]	Antenna array	Two 6-way dividers + phase-shift networks	$6 \times 8 = 48$	$5.2 \times 6.9 \times 0.24$	22.2
[15]	Antenna array	Cascaded SIW 1-to-64 divider	$8 \times 8 = 64$	$6.53 \times 6.53 \times 0.7$	26.8
[16]	Antenna array	Gap waveguide corporate feed	$8 \times 8 = 64$	$8 \times 8 \times 1.1$	28
[17]	Fabry–Perot	PRS cavity feed	1	$2.5 \times 2.5 \times 1.4$	12.89
[18]	Fabry–Perot	PRS cavity feed (circular)	1	$4.8 \times 4.8 \times 1.0$	17.2
[19]	Fabry–Perot	PRS cavity feed	1	$2.6 \times 2.6 \times 0.5$	13.4
[20]	Fabry–Perot	PRS cavity feed	1	$6.5 \times 6.5 \times 0.5$	22.6
Proposed	**Single element**	**Branch-line hybrid coupler (90°)**	**1**	$1.49\,\lambda \times 1.49\,\lambda \times 0.04$	**12.3**

REFERENCES

[1] W. Cao, A. Liu, B. Zhang, T. Yu, and Z. Qian, "Dual-band spiral patch-slot antenna with omnidirectional cp and unidirectional cp properties," *IEEE Transactions on Antennas and Propagation*, vol. 61, no. 4, pp. 2286–2289, 2013. doi: 10.1109/TAP.2012.2235400

[2] F. Zhang, G.-M. Yang, Y.-Q. Jin, F. Peng, and J. Mo, "Space-borne deployable p-band dual-circular-polarization flexible antenna array," *IEEE Antennas and Wireless Propagation Letters*, vol. 16, pp. 2529–2533, 2017. doi: 10.1109/lawp.2017.2731052

[3] S. Wang, L. Zhu, and W. Wu, "3-d printed inhomogeneous substrate and superstrate for application in dual-band and dual-cp stacked patch antenna," *IEEE Transactions on Antennas and Propagation*, vol. 66, no. 5, pp. 2236–2244, May 2018. doi: 10.1109/tap.2018.2810330

[4] M. Wang, D.-Y. Wang, W. Wu, and D.-G. Fang, "Single-layer, dual-port, dual-band, and orthogonal-circularly polarized microstrip antenna array with low frequency ratio," *Wireless Communications and Mobile Computing*, vol. 2018, no. 1, Jan. 2018. doi: 10.1155/2018/5391245

[5] Z. Zhao, F. Liu, J. Ren, Y. Liu, and Y. Yin, "Dual-sense circularly polarized antenna with a dual-coupled line," *IEEE Antennas and Wireless Propagation Letters*, vol. 19, no. 8, pp. 1415–1419, Aug. 2020. doi: 10.1109/lawp.2020.3003943

[6] W. Wang, H. Jin, W. Yu, X. H. Zhang, F. Wu, K.-S. Chin, and G. Q. Luo, "A single-layer dual-circularly polarized siw-cavity-backed patch filtenna with wide axial-ratio bandwidth," *IEEE Antennas and Wireless Propagation Letters*, vol. 20, no. 6, pp. 908–912, 2021. doi: 10.1109/LAWP.2021.3066616

[7] I. Mujahidin and A. Kitagawa, "Cp antenna with 2 × 4 hybrid coupler for wireless sensing and hybrid rf solar energy harvesting," *Sensors*, vol. 21, no. 22, p. 7721, Nov. 2021. doi: 10.3390/s21227721

[8] A. H. Mohammed, F. M. Alnahwi, and Y. I. A. Al-Yasir, "A circularly polarized microstrip antenna with dual circular polarization using a 90° hybrid coupler and proximity-coupled feeding for lte 43 5g applications," *Applied Sciences*, vol. 14, no. 24, p. 11877, Dec. 2024. doi: 10.3390/app142411877

[9] H. H. Tran and I. Park, "Wideband circularly polarized 2 × 2 antenna array with multibeam steerable capability," *IEEE Antennas and Wireless Propagation Letters*, vol. 16, pp. 345–348, 2017. doi: 10.1109/lawp.2016.2576019

[10] W. Yang, Q. Meng, W. Che, L. Gu, and Q. Xue, "Low-profile wide-band dual-circularly polarized metasurface antenna array with large beamwidth," *IEEE Antennas and Wireless Propagation Letters*, vol. 17, no. 9, pp. 1613–1616, Sep. 2018. doi: 10.1109/lawp.2018.2857625

[11] S. Gupta, A. Sharma, G. Das, R. K. Gangwar, and M. Khalily, "Wideband circularly polarized dielectric resonator antenna array with polarization diversity," *IEEE Access*, vol. 7, pp. 49 069–49 076, 2019. doi: 10.1109/access.2019.2909581

[12] M. Jafari Chashmi, P. Rezaei, A. H. Haghparast, and D. Zarifi, "Dual circular polarization 2 × 2 slot array antenna based on printed ridge gap waveguide technology in ka band," *AEU - International Journal of Electronics and Communications*, vol. 157, p. 154433, Dec. 2022. doi: 10.1016/j.aeue.2022.154433

[13] C. Zhu, G. Xu, A. Ren, W. Wang, Z. Huang, and X. Wu, "A compact dual-band dual-circularly polarized siw cavity-backed antenna array for millimeter-wave applications," *IEEE Antennas and Wireless Propagation Letters*, vol. 21, no. 8, pp. 1572–1576, Aug. 2022. doi: 10.1109/lawp.2022.3174419

[14] J.-D. Zhang, L. Zhu, N.-W. Liu, and W. Wu, "Dual-band and dual-circularly polarized single-layer microstrip array based on multiresonant modes," *IEEE Transactions on Antennas and Propagation*, vol. 65, no. 3, pp. 1428–1433, Mar. 2017. doi: 10.1109/tap.2016.2647582

[15] Y. Zhao and K.-M. Luk, "Dual circular-polarized siw-fed high-gain scalable antenna array for 60 ghz applications," *IEEE Transactions on Antennas and Propagation*, vol. 66, no. 3, pp. 1288–1298, Mar. 2018. doi: 10.1109/tap.2018.2797530

[16] M. Ferrando-Rocher, J. I. Herranz-Herruzo, A. Valero-Nogueira, and B. Bernardo-Clemente, "Dual circularly polarized aperture array antenna in gap waveguide for high-efficiency ka-band satellite communications," *IEEE Open Journal of Antennas and Propagation*, vol. 1, pp. 283–289, 2020. doi: 10.1109/ojap.2020.3001087

[17] R. Huang, Z. Wang, G. Li, C. Lin, Y. Ge, and J. Pu, "A metasurface-enabled wideband high-gain dual-circularly-polarized fabry-perot resonator antenna," *Microwave and Optical Technology Letters*, vol. 62, no. 10, pp. 3195–3202, May 2020. doi: 10.1002/mop.32422

[18] Y.-L. Li and K.-M. Luk, "Dual circular polarizations generated by self-polarizing fabry–pérot cavity antenna with loaded polarizer," *IEEE Transactions on Antennas and Propagation*, vol. 69, no. 12, pp. 8890–8895, Dec. 2021. doi: 10.1109/tap.2021.3090850

[19] Y. Wang and A. Zhang, "Dual circularly polarized fabry–perot resonator antenna employing a polarization conversion metasurface," *IEEE Access*, vol. 9, pp. 44 881–44 887, 2021. doi: 10.1109/access.2021.3062460

[20] J. Li and X. Huang, "Dual circular polarization fabry–pérot resonant antennas based on meta-surface," *Electronics*, vol. 12, no. 1, p. 173, Dec. 2022. doi: 10.3390/electronics12010173

[21] Q. Umar Khan, M. Bin Ihsan, D. Fazal, F. Mumtaz Malik, S. A. Amin, and S. Masuad, "Higher order modes: A solution for high

gain, wide band patch antennas for different vehicular applications," *IEEE Transactions on Vehicular Technology*, pp. 1–1, 2016. doi: 10.1109/tvt.2016.2604004

[22] J.-Y. Yang, X.-H. Ding, T.-Y. Yan, W.-W. Yang, Y. Li, and J.-X. Chen, "High-gain 60 ghz high-order-mode patch antenna array based on single-layer ridge gap waveguide," *IEEE Antennas and Wireless Propagation Letters*, vol. 24, no. 4, pp. 878–882, Apr. 2025. doi: 10.1109/lawp.2024.3520112

[23] H. Nguyen-Huy, D.-N. Tran-Viet, P. Kim-Thi, and H. Tran-Huy, "Compact high-gain circularly polarized patch antenna based on tm30/tm03 mode," *PLOS One*, vol. 20, no. 5, p. e0321091, 5 2025. doi: 10.1371/journal.pone.0321091

[24] H. Tran-Huy and T. Pham-Danh, "Low-profile high-gain circularly polarized antenna using high-order mode microstrip patch," *Heliyon*, vol. 11, no. 9, p. e42863, Apr. 2025. doi: 10.1016/j.heliyon.2025.e42863

[25] C. A. Balanis, *Antenna Theory: Analysis and Design*, 4th ed. New York, NY, USA: Wiley, 2005.

Dieu Nguyen-Khanh is currently an undergraduate student in Biomedical Engineering at Phenikaa University, Vietnam. Some of her research works have been published and presented at several national and international scientific conferences, including RIVF, REV, and ICCE. Her research interests include antenna design, compact antenna structures, and applications of antennas in biomedical engineering.

Dat Nguyen-Tien received the B.S. degree in electronics and telecommunications from HUST,Hanoi, Vietnam, in 2009, and the Ph.D. degree in electronics and electrical engineering from Dong-guk University, in 2015. He had been a Professor with the Division of Electronics and Electrical Engineering, Dongguk University, since March 2015 to Feb, 2023. From 2023, He has been with Phenikaa University. His research interests include image processing, biometrics, and deep learning. He supervised this research and revised the original article.

Nguyen Tran received a B.S. degree in Communication Command at Telecommunications University, Vietnam, in 2011. He received his M.S. degree in Electronics Engineering from Le Quy Don Technical University, Vietnam in 2017. He is currently an Assistant with Phenikaa University, Hanoi, Vietnam. His research interests are centered on antenna design and RF engineering, specifically focusing on the optimization of microstrip patch antennas and the development of wideband systems. His work also explores the implementation of circular polarization, metasurfaces for bandwidth enhancement on MIMO antennas.

Thai Dinh Nguyen received a B.S. degree in Communication Command at Telecommunications University, Vietnam, in 2010. He received his M.S. degree in Telecommunication Engineering from Posts and Telecommunications Institute of Technology, Vietnam in 2021. He is currently pursuing a Ph.D degree at Le Quy Don Technical University, Hanoi, Vietnam. His research interests have included reconfigurable antennas, MIMO antennas, and metamaterial-based antennas.

Niamat Hussain (Senior Member, IEEE) is a Lecturer (Assistant Professor) at the Division of Electronics and Nanoscale Engineering, James Watt School of Engineering, University of Glasgow, UK. Previously, he worked as an Assistant Professor in Intelligent Mechatronics Engineering at Sejong University, Korea (2022–2024). Dr. Niamat's research expertise spans Antenna Engineering, including mm-wave and THz antennas, metasurface and beam-forming antennas; Microwave Engineering, such as wireless power transfer and Reflecting Intelligent Surfaces, and metamaterials; and Bioelectromagnetics, focusing on SAR reduction in wearable devices and the health effects of electromagnetic fields. Dr. Niamat's work has been recognized globally. He has been featured among the World's Top 2% Scientists (2021–2023) by Stanford University and received numerous other awards, including an endorsement as a UK Exceptional Talent in the field of Applied Electromagnetics, awarded to early-career world-leading innovators and scientists by the Royal Academy of Engineering under the UKBA Tier 1 program. Dr. Niamat is actively involved in professional activities, serving as an Associate Editor of the IEEE Internet of Things Journal, editorial board member for Electronics, Micromachines, IET Microwaves, Antennas, and Propagation, and guest editor for multiple prestigious journals. He is a senior member of IEEE and several professional societies, including the European Bioelectromagnetic Society, the Korean Society of Electromagnetic Engineering and Science, and a Member of the Evaluation Committee for National Research and Development Projects in South Korea. His research is dedicated to advancing technology with a strong focus on societal and environmental benefits.

Hung Tran-Huy received the B.S. degree in electronics and telecommunications from Hanoi University of Science and Technology, Hanoi, Vietnam, in 2013. He received his M.S. and Ph. D. degrees in electrical engineering from Ajou University, in 2015, and Dongguk University, Korea, in 2020, respectively. He is currently a lecturer at Faculty of Electrical and Electronic Engineering, PHENIKAA School of Engineering, PHENIKAA University, Hanoi, Vietnam. His research interests have included circularly polarized antennas, MIMO antennas, metamaterial-based antennas, and reconfigurable antennas.